Science of the Total Environment 544 (2016) 617–626

Contents lists available at ScienceDirect

Science of the Total Environment

journal homepage: www.elsevier.com/locate/scitotenv

Spatiotemporal trends of urban heat island effect along the urban development intensity gradient in China

Decheng Zhou [a,*], Liangxia Zhang [a], Lu Hao [a], Ge Sun [b], Yongqiang Liu [c], Chao Zhu [d]

[a] Jiangsu Key Laboratory of Agricultural Meteorology, College of Applied Meteorology, Nanjing University of Information Science and Technology, Nanjing 210044, China
[b] Eastern Forest Environmental Threat Assessment Center, Southern Research Station, USDA Forest Service, Raleigh, NC 27606, USA
[c] Center for Forest Disturbance Science, Southern Research Station, USDA Forest Service, Athens, GA 30602, USA
[d] Nanjing Institute of Environmental Sciences of the Ministry of Environmental Protection of PR China, Nanjing, Jiangsu 210042, China

HIGHLIGHTS

- Spatiotemporal trends of the UHI effect (ΔT) were analyzed in China.
- ΔT varied greatly across cities, UDI zones, and time periods.
- ΔT–UDI patterns were mostly in linear form except few convex or concave ones.
- ΔT increased or remained stable from 2003 to 2012 for most cities.
- Caution should be paid to the methods to quantify UHI intensity over large areas.

GRAPHICAL ABSTRACT

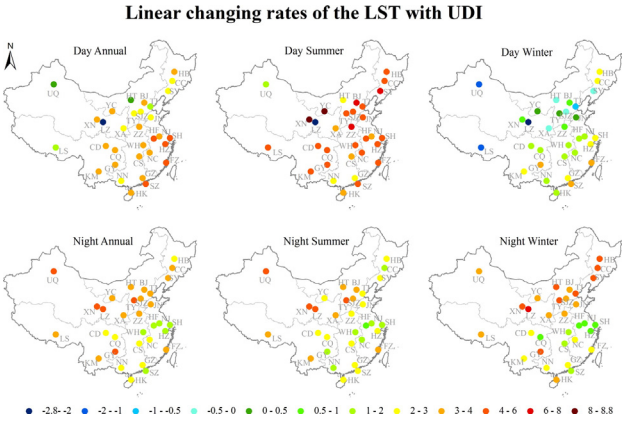

ARTICLE INFO

Article history:
Received 8 July 2015
Received in revised form 24 November 2015
Accepted 29 November 2015
Available online xxxx

Editor: Simon Pollard

Keywords:
Urbanization
Urban heat island
Spatiotemporal variations
Background climate
Land use activities
MODIS

ABSTRACT

Urban heat island (UHI) represents a major anthropogenic modification to the Earth system and its relationship with urban development is poorly understood at a regional scale. Using Aqua MODIS data and Landsat TM/ETM + images, we examined the spatiotemporal trends of the UHI effect (ΔT, relative to the rural reference) along the urban development intensity (UDI) gradient in 32 major Chinese cities from 2003 to 2012. We found that the daytime and nighttime ΔT increased significantly ($p < 0.05$, mostly in linear form) along a rising UDI for 27 and 30 out of 32 cities, respectively. More rapid increases were observed in the southeastern and northwestern parts of China in the day and night, respectively. Moreover, the ΔT trends differed greatly by season and during daytime in particular. The ΔT increased more rapidly in summer than in winter during the day and the reverse occurred at night for most cities. Inter-annually, the ΔT increased significantly in about one-third of the cities during both the day and night times from 2003 to 2012, especially in suburban areas ($0.25 < UDI \leq 0.5$), with insignificant trends being observed for most of the remaining cities. We also found that the ΔT patterns along the UDI gradient were largely controlled by local climate-vegetation conditions, while that across years were dominated by human activities. Our results highlight the strong and highly diverse urbanization effects on local climate cross China and offer limitations on how these certain methods should be used to quantify UHI intensity over large areas. Furthermore, the impacts of urbanization on climate are complex, thus future research efforts should focus more toward direct observation and physical-based modeling to make credible predictions of the effects.

* Corresponding author at: No. 219, Ningliu Road, Nanjing, Jiangsu, P. R. China 210044
E-mail address: zhoudc@nuist.edu.cn (D. Zhou).

http://dx.doi.org/10.1016/j.scitotenv.2015.11.168
0048-9697/

1. Introduction

Urbanization is accelerating in the world. More than half of world's population live in urban areas now, and this number is projected to be 66% by 2050 (United Nations, 2014). At the same time, the amount of global urban land is expanding at twice the population growth rate (Angel et al., 2011) and is expected to nearly triple by 2030 if current trends in population density continues (Seto et al., 2012). Urban heat island (UHI) phenomenon, referred as the temperature rise in urban relative to surrounding areas (Oke, 1973; Arnfield, 2003), is one of the most important urbanization-induced impacts. It cannot only alters environmental conditions such as net primary production (Imhoff et al., 2004; Zhou et al., 2014a), biodiversity (Reid, 1998), water and air quality (Grimm et al., 2008), and climate (Arnfield, 2003; Dixon and Mote, 2003; IPCC, 2014; Jin et al., 2005; Shepherd, 2005) but also can affect human health and comfort (Gong et al., 2012; Patz et al., 2005). These effects are expected to be more serious when interacting with global climate changes (IPCC, 2014; Patz et al., 2005). Thus a better understanding of the UHI effects is important to support future climate change mitigation and human adaptive strategies (Arnfield, 2003; Imhoff et al., 2010; Zhou et al., 2014b).

The UHI effect could undergo changes during urban development mainly in two opposite ways. On one hand, an increase in the proportion of impervious surface (built-up land) reduces the vegetated areas and can elevate the UHI effect due to the resultant decrease in latent heat flux and the increase in heat storage (Arnfield, 2003). On the other hand, several approaches or conditions have been reported to able to mitigate or alleviate the UHI effect. For example, the management of urban green spaces (e.g., fertilization, irrigation, and green space creation) has been shown to largely offset the negative effects associated with land cover change from rural to urban conditions (Gregg et al., 2003; Searle et al., 2012). In addition, a reduction in incoming solar radiation has been reported due to heavy smoke over urban areas (Oke, 1982; Sang et al., 2000).

However, a systematic evaluation on the spatiotemporal trends of the UHI effects along an urban development intensity (UDI) gradient across multiple cities is still lacking. Relatively limited studies focused on the spatial trends or site-specific observations. For example, Yuan and Bauer (2007) found a strong linear relationship between land surface temperature (LST) and percent impervious surface (can be considered as a surrogate for UDI) in the Twin Cities of Minnesota. Imhoff et al. (2010) examined the general relationship between UHI and UDI for 38 most populous cities in the continental United States, but paid little attention to the spatiotemporal variability of the correlations. Since the UHI intensity (Clinton and Gong, 2013; Peng et al., 2012; Zhou et al., 2014b) and the vegetation dynamics (one major driver for the UHI effect) (Zhou et al., 2014a) varied substantially across space and time, there is a strong impetus to systematically understand the UHI spatiotemporal patterns in parallel with rapid urbanization.

In this study, we analyzed the UHI effects from 2003 to 2012 for 32 major cities across various climatic regions of China using Moderate Resolution Imaging Spectoradiometer (MODIS) land surface temperature (LST) products in conjunction with Landsat Thematic Mapper (TM) and Enhanced Thematic Mapper Plus (ETM +) images. Unlike our previous efforts that focused on UHI intensity (urban–suburban LST differences) (Zhou et al., 2014b) and the footprint of the UHI effects (Zhou et al., 2015), the purposes of this study were to (1) investigate the relationship between UHI and UDI and (2) examine the temporal trends of the UHI effect in parallel with rapid urbanization of those cities. China is ideal to investigate the climatic effects induced by urbanization at a regional scale, since it has being experienced the fastest urbanization in the world in the past three decades (United Nations, 2014; Seto et al., 2012) and has a climate ranging from tropical to subarctic/alpine and from rain forest to desert. Analyzing UHI effects in China can not only help enhance understanding the physical characteristics and driving forces of UHI in general, but can also be essential for formulating climate mitigation strategies and long-term ecosystem management plans in the country.

2. Materials and methods

2.1. Remotely sensed land surface temperature (LST) and urban development intensity (UDI)

All 32 cities are municipalities or provincial capitals except Shenzhen, which is China's first special economic zone and was established in 1978. It is now considered as one of the fastest growing cities in the world (Fig. 1). Most cities are mainly surrounded by cultivated land and the rest by forests (e.g., Hangzhou and Fuzhou) or grassland (Lhasa). The maximal research areas of these cities were defined by China's official administrative areas (i.e., city, *shi*) (Chan, 2010). Water body pixels within the administrative boundaries or those with an elevation more than 50 m above the highest point in urban and urban core zones (see definition below) were excluded from this analysis (Figs. 1 and 2) because these pixels may overshadow the urbanization effects on temperature (Imhoff et al., 2010; Zhou et al., 2015).

LST was obtained from Aqua MODIS 8-days composite products (version 5) with a spatial resolution of 1 km (MYD11A2) from 2003 to 2012. The LST data, including temperature observations that were monitored at 13:30 h (daytime) and 1:30 h (nighttime) local solar time, were estimated using a generalized split-window algorithm (Wan and Dozier, 1996). The retrieval of LST was further improved by correcting noise resulting from cloud contamination, topographic differences, and zenith angle changes, with the absolute bias generally less than 1 K and less than 0.5 K in most cases (Wan, 2008).

Land cover maps of each city were derived from the cloud-free Landsat TM images (downloaded free from http://www.usgs.gov/) with a spatial resolution of 30 m. The gap-filled Landsat ETM + Scan Line Corrector (SLC)-off products (obtained free from http://www.gscloud.cn/) were used instead for few cases provided without the TM data. The scan gaps were filled using a local linear histogram matching technique (Storey et al., 2005). Around 170 scenes of images were used to extract the extent of urban land for all the cities in this study (Table S1). The acquisition time of these images spanned 2004–2006 and 2009–2011 and represented two time periods of circa 2005 and 2010, respectively. The land covers were classified into four broad types (i.e., built-up land, water body, cultivated land, and other land) using the maximum likelihood classification approach (Strahler, 1980). The accuracies of the classified products were assessed by using the high-resolution images and pictures incorporated in Google Earth Pro®. The accuracies, measured by Kappa coefficients (Foody, 2002), were generally larger than 0.80 for all those cities. Details on land use classification can be found in Zhao et al. (2015).

UDI was defined as the proportion of built-up areas in each MODIS LST pixel in this analysis. It was mapped using 33 × 33 moving window based on the 30 m urban land cover maps for the year 2005 and 2010 for each city individually. The resultant UDI map has a spatial resolution of 990 m and was resampled to 1 km in order to keep accordance with the size of LST data. We further stratified the landscape into five zones based on the UDI. Emanating inward from the lowest to the highest UDI in a city (Fig. 2), these five zones were rural ($UDI \le 0.05$) and four urban zones [exurban ($0.05 < UDI \le 0.25$), suburban ($0.25 < UDI \le 0.5$), urban ($0.5 < UDI \le 0.75$), and urban core ($0.75 < UDI \le 1$)]. The rural area was usually covered by both cultivated and natural vegetation, while the exurban and suburban areas were mainly covered by cultivated vegetation besides built-up land (Fig. 1).

2.2. Trends of UHI effect along the UDI gradients

The mean LST in the five UDI zones were calculated over the period 2003–2012. For the years without UDI maps, we assumed that the UDI maps in 2005 and 2010 can be applied to 2003–2007 and 2008–2012,

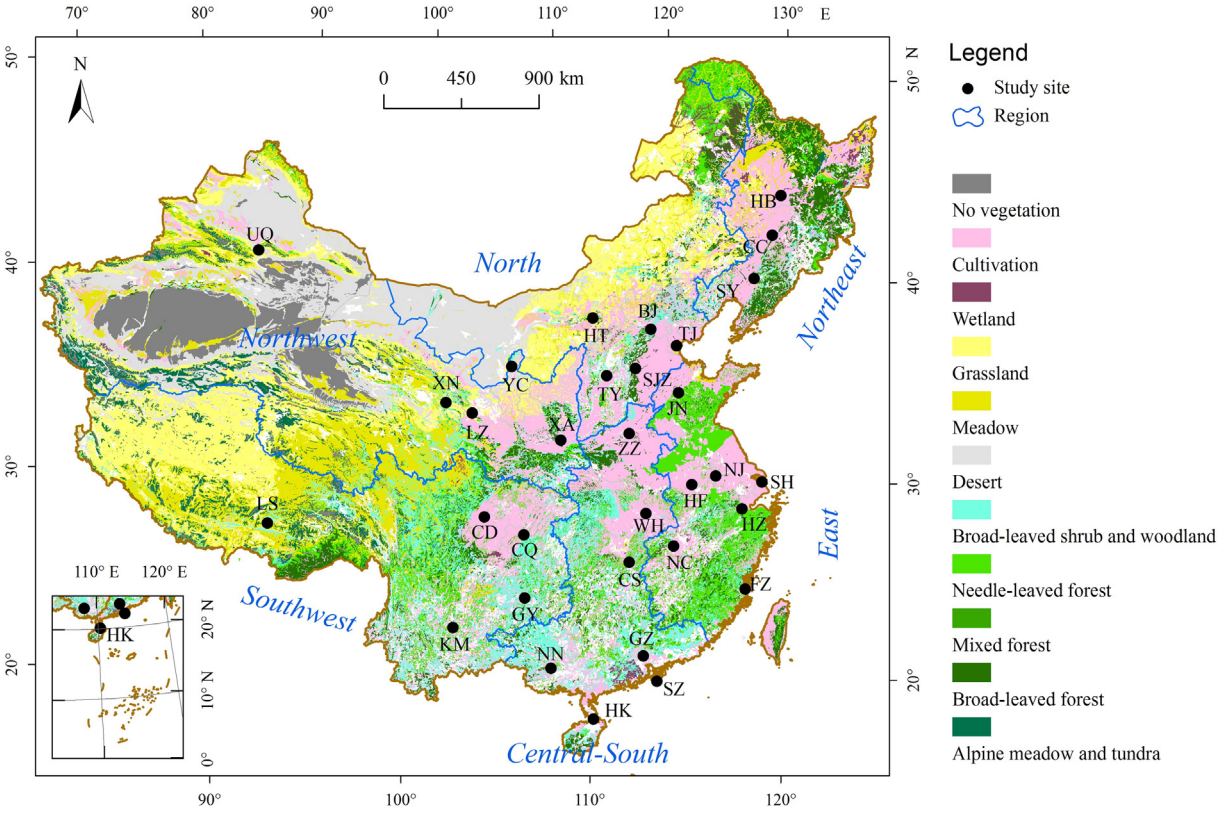

Fig. 1. Locations of the 32 major cities and six regions in China, with the background map indicating the vegetation map of China (this data set is provided by "Environmental& Ecological Science Data Center for West China, National Natural Science Foundation of China" (http://westdc.westgis.ac.cn)). All the sites are provincial capitals or provincial/autonomous regional capitals except Shenzhen, which is China's first special economic zone and is now considered one of the fastest growing cities in the world. BJ: Beijing; CC: Changchun; CS: Changsha; CD: Chengdu; CQ: Chongqing; FZ: Fuzhou; GZ: Guangzhou; GY: Guiyang; HK: Haikou; HZ: Hangzhou; HB: Harbin; HF: Hefei; HT: Hohhot; JN: Jinan; KM: Kunming; LZ: Lanzhou; LS: Lhasa; NC: Nanchang; NJ: Nanjing; NN: Nanning; SH: Shanghai; SY: Shenyang; SZ: Shenzhen; SJZ: Shijiazhuang; TY: Taiyuan; TJ: Tianjin; UQ: Urumqi; WH: Wuhan; XA: Xi'an; XN: Xining; YC: Yinchuan; ZZ: Zhengzhou. Map was generated using ArcGIS 9.3 (www.esri.com/software/arcgis).

respectively. The dynamic urban coverage maps were used to delineate rural and urban areas for each city in order to reflect the actual UHI trends along the UDI gradient impacted by rapid urban expansion. For example, the urban areas for the 32 cities increased by 44% on average between 2005 and 2010 (data not shown). We hypothesized that there was no UHI effect in rural areas that can be considered as the reference. The UHI effect was then estimated as the temperature differences relative to rural areas (ΔT). The annual and seasonal (summer and winter) ΔT in the day (13:30) and night (1:30) were calculated over the period 2003–2012 for each city individually. Summer and winter were defined as the periods from June to August, and from December to February, respectively. Linear regression analysis was performed to examine the increasing rate of the ΔT with a rising UDI for each city. To investigate the spatial variability of the ΔT trends across cities in China, we estimated the linear rates of the ΔT along the UDI gradients in all six sub-regions of China. Significance tests ($p = 0.05$) were conducted to determine if there were differences across regions.

We explored the climatic effects on the spatial variability of the ΔT increasing rates across cities. Annual climate data of precipitation and temperature from 2003 to 2012 for each city were obtained from China Meteorological Observation (downloaded free from http://cdc.cma.gov.cn/). The impacts of background vegetation conditions, reflected by rural enhanced vegetation index (EVI), were also assessed with the hypothesis that the city with a larger EVI should have a greater ΔT increasing rate (Peng et al., 2012; Zhou et al., 2014b). The version-5 Terra MODIS EVI (MOD13A2) between 2003 and 2012 was used in this

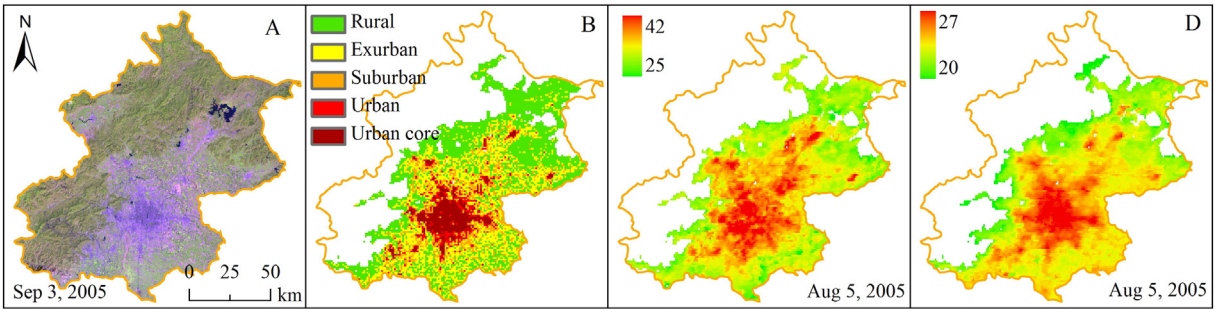

Fig. 2. Beijing area maps of (A) Landsat TM true color image acquired in Sep. 3, 2005 with a spatial resolution of 30 m, (B) regions with different urban development intensity (UDI) that was derived from urban land cover map (i.e., rural, $UDI < 0.05$; exurban, $UDI = 0.05–0.25$; suburban, $UDI = 0.25–0.5$; urban, $UDI = 0.5–0.75$; urban core, $UDI > 0.75–1$), (C) annual mean daytime land surface temperature (LST, °C), and (D) annual mean nighttime LST. The blank areas on the map were not included in the analysis, which were either water bodies or the areas excluded by elevation consideration.

analysis (1 km spatial resolution and 16-day interval). Noises caused by cloud contamination, atmospheric variability, and bi-directional effects were further removed using an adaptive Savitzky–Golay filtering method (Chen et al., 2004; Jönsson and Eklundh, 2004; Zhou et al., 2014a). The Pearson's correlation analyses were performed in SPSS PASW Statistics 18 (SPSS Inc.).

2.3. Temporal trends of UHI effect in different urban zones

In order to examine the UHI trends over time induced by rapid urbanization, the annual mean ΔT rates were estimated for the period 2003–2012 using the static UDI zones of the year 2005. The UHI effect in an urban zone was assumed constant if an insignificant ΔT trend over time was observed. Linear regression models were used to test for temporal patterns of the ΔT for each city separately. We also evaluated the temporal trends of rural LST using linear regression to examine the possible temperature changes induced by climate variability and human activities (e.g., tree planting or deforestation, and cropland management). The Pearson's correlation coefficients between climatic factors (annual mean temperature and annual precipitation) and ΔT in urban zones were calculated for each city in order to investigate the responses of the ΔT to climate variability.

3. Results

3.1. Spatial trends of UHI effects with rising UDI

The area-weighted annual mean UHI effect (ΔT) averaged from 2003 to 2012 increased significantly ($p < 0.05$) with rising UDI for 27 out of 32 cities during the daytime (Figs. 3 and 4). The ΔT–UDI trends in five arid/semi-arid cities (Urumqi, Lhasa, Lanzhou, Hohhot, and Taiyuan) were not statistically significant (Fig. 4A). In particular, an evident decay trend happened in Lanzhou, while a slight decrease after an increase occurred in Taiyuan (Fig. 3). The significant ΔT increasing rates (reflected by the linear regression slope between ΔT and UDI) varied greatly with geographic locations from 1.7 in Tianjin to 5.1 in Fuzhou (Fig. 4A). Overall, the cities located in the southeastern parts of China (East, Central-south, and Southwest China) experienced more rapid increase compared to northwestern counterparts (Northwest, North, and Northeast China) (Figs. 4A and 5A). Comparatively, the annual mean nighttime ΔT increased significantly ($p < 0.05$) with UDI for 30 out of 32 cities except two humid hot cities (Nanjing and Hefei) (Figs. 4D and 6). Cold island effects (i.e., negative ΔT) were observed in exurban and suburban areas relative to rural reference for Nanjing and Hefei (Fig. 6). The significant ΔT increasing rates varied substantially from 1.1 °C (per 100% UDI, hereafter) in Shanghai to 5.4 °C in Lanzhou, with the largest in Northwest China (4.3 ± 1.0 °C, mean ± standard deviation) and the least in East China (2.0 ± 0.7 °C) (Figs. 4D and 5D). For all cities combined, the annual mean rate was 2.9 ± 0.8 °C in the day and 3.1 ± 0.5 °C at night (Fig. 5A and D).

The ΔT–UDI trends differed greatly by season. The daytime ΔT increased more rapidly in summer than in winter for nearly all the cities (Figs. 3, 4B, and C). All cities except for Lanzhou (insignificant decrease) and Hohhot (insignificant increase with cold island effect in exurban and suburban areas) exhibited evident increases in summer, whereas about half of the cities had insignificant trends (mostly decrease) in winter. On average, the increasing rate reached up to 4.7 ± 0.7 °C in summer, over four times that in winter (1.1 ± 0.6 °C). The northern parts of China witnessed more obvious seasonal changes compared to southeastern neighbors (Fig. 5B and C). Interestingly, the ΔT declined after an increase with a rising UDI in Urumqi in summer, whereas the opposite happened in winter. The ΔT increased linearly from exurban to urban core in summer, and the reverse occurred in winter for Hohhot. By contrast, the nighttime ΔT–UDI trends differed slightly by season, characterized by the average rates of 2.7 ± 0.6 °C and 3.1 ± 0.7 °C across cities in summer and winter, respectively. Cities in Northeast and North China presented more evident trends in winter than summer, while that in other regions varied slightly by season.

Notably, a clear concave or convex increase was observed in few cities. Specifically, the concave increases occurred in Changchun, Jinan, Shenyang, Shijiazhuang, and Tianjin in the day during summer, and in Changchun, Harbin, Jinan, Shenyang, Shijiazhuang, and Xi'an at night in both summers and winters. By contrast, the convex increases were found in Kunming and Shenzhen in the day, and in Lanzhou and Lhasa at night in both seasons.

The daytime ΔT increasing rates were positively and significantly ($p < 0.01$) related to mean annual temperature and precipitation in winters, but were negatively (statistically insignificant) linked to both

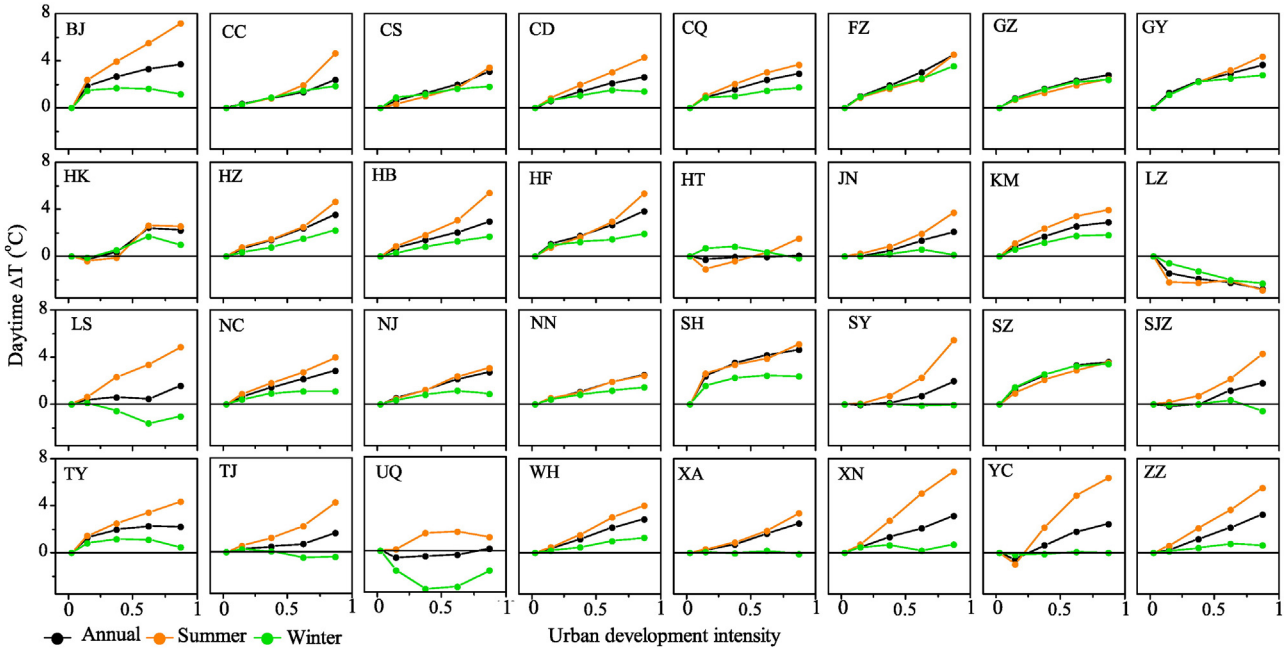

Fig. 3. Trends of daytime urban heat island effect (ΔT, defined as the LST differences relative to rural areas) with UDI for China's 32 major cities averaged over 2003–2012. Summer and winter were defined as the periods from June to August, and from December to February, respectively.

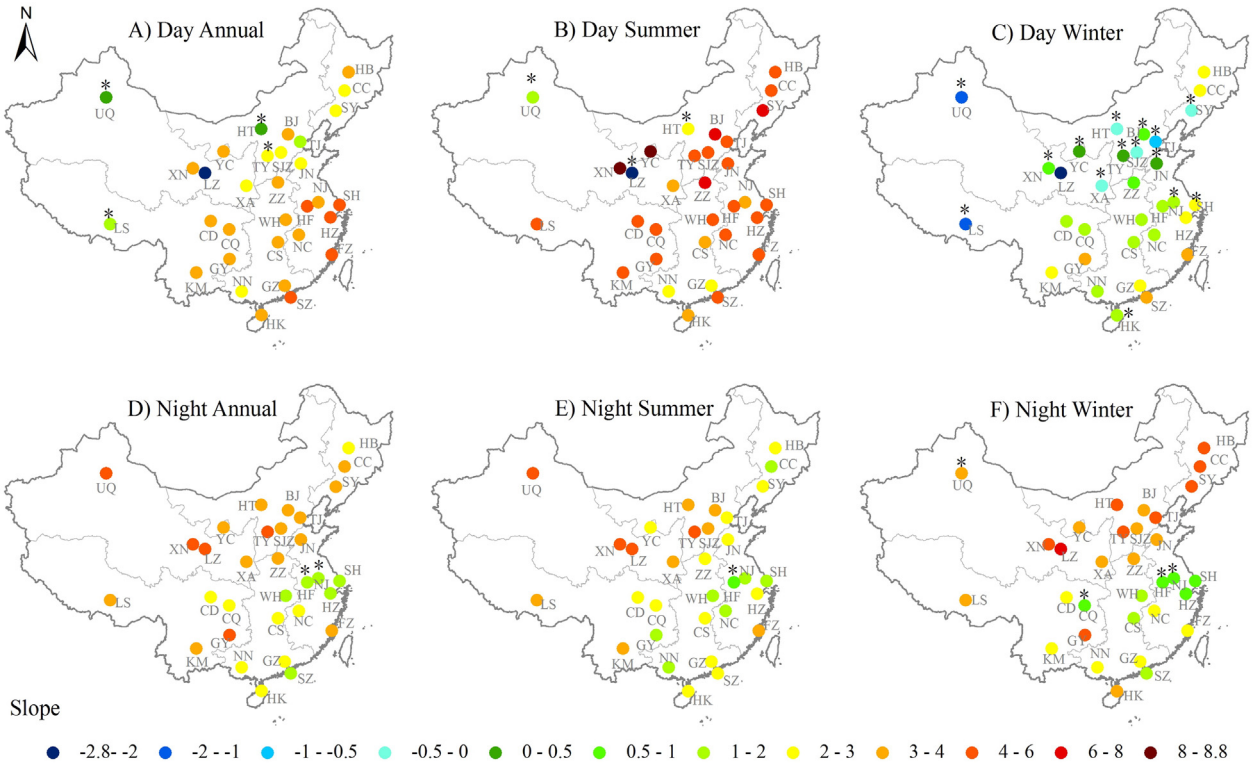

Fig. 4. Spatial distribution of the linear changing rates of the LST along UDI gradients for China's 32 major cities. * indicates an insignificant linear trend at the 0.05 level.

variables in summers (Table 1). In contrast, the nighttime ΔT increasing rates were negatively ($p < 0.01$) related to mean annual temperature and precipitation in both summer and winter seasons. Moreover, the background vegetation condition, as reflected by rural EVI, was positively and negatively related to daytime and nighttime ΔT increasing rates in both seasons ($p < 0.05$), respectively.

3.2. Temporal trends of UHI effects in different urban zones

The temporal trends of the ΔT differed greatly across urban zones and cities from 2003 to 2012 (Table 2). Relative to the rural base condition, the annual mean daytime ΔT increased significantly ($p < 0.05$) over 8, 12, 5, and 2 out of 32 cities in exurban, suburban, urban, and urban core areas, respectively. Comparatively, the ΔT elevated significantly over 6, 12, 10, and 8 cities in exurban, suburban, urban, and urban core areas at night, respectively. Concurrently, evident decline trends were observed in three cities of urban (Hohhot, Lhasa, and Shanghai) and urban core zones (Hohhot, Shanghai, and Xining), and one city of exurban (Changchun) and suburban (Hohhot) areas during the day. By contrast, only the exurban of Yinchuan showed apparent ($p < 0.05$) decay trends during the night. Interestingly, the reference rural LST reduced significantly in about 10 out of 32 cities during both the day and night time periods.

The inter-annual variations of rural LST were positively related to annual mean air temperature for majority of cities in both the day (significant for 19 of 32) and night (significant for 18 of 32) (Table S2). At the same time, the rural LST was negatively linked with annual precipitation for most cities, whereas significantly for only eight and one city during the day and night, respectively. Comparatively, both the positive and negative relations were observed between the inter-annual variations of the ΔT in urban zones (exurban, suburban, urban, and urban core) and annual mean air temperature or precipitation, although the correlations were significant for few cities only (Table S2). For example, the ΔT related positively and significantly ($p < 0.05$) to annual precipitation in some urban zones of five cities (e.g., Beijing, Shijiazhuang, Hangzhou, Lanzhou, Xining, and Lhasa) during the day, and two cities (Beijing and Hefei) at night. Concurrently, the significant negative correlations were observed in three cities (Changchun, Urumqi, and Shenzhen) during the day, and five cities (Xi'an, Fuzhou, Nanchang, Guangzhou, and Lhasa) at night. Similar

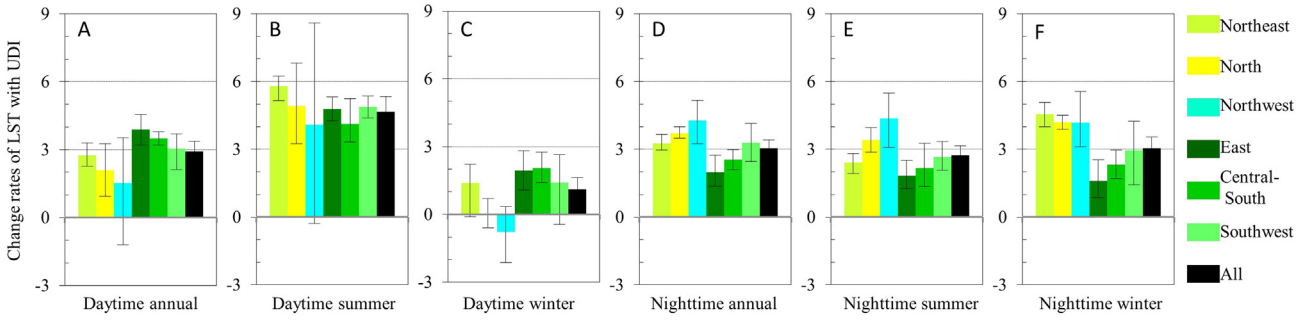

Fig. 5. Mean linear changing rates of the LST along the UDI gradients (mean ± standard deviation) during the day and night in different regions of China.

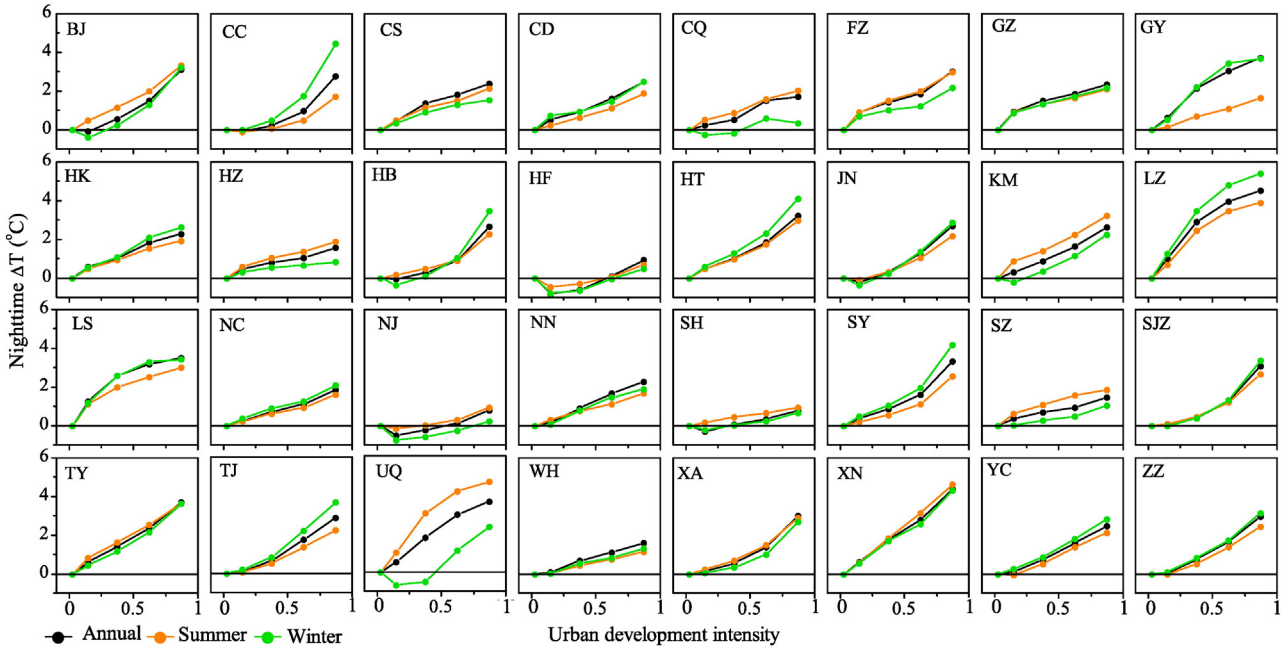

Fig. 6. Trends of nighttime ΔT with UDI for China's 32 major cities averaged over 2003–2012.

phenomenon happened for the relationships with annual mean air temperature (Table S2).

4. Discussion

4.1. Spatial relationship between UHI and UDI in China and their drivers

Our results showed that the UHI effect (i.e., ΔT) increased significantly with rising UDI for most of the cities in the day and night (Figs. 3–6), which is consistent with findings in the United States (Imhoff et al., 2010) and other synthesis reports (Arnfield, 2003). The ΔT increasing rate was apparently weaker (even insignificant for few cities) in arid–cold regions (i.e., the northern parts of China) during the day, mostly owing to the low vegetation activity in these dry areas compared to the other regions. For example, the background vegetation conditions (as reflected by rural EVI) in Central-south China was over 1.7 times that in Northwest China (0.36 vs. 0.21). This phenomenon can be further verified by the strong positive correlation between ΔT increasing rates and rural EVI across cities in the daytime (Table 1).

In contrast, low ΔT increasing rates were found in humid–hot cities at night, which can be explained by their high soil moisture and the low surface albedo in the regions (Zhou et al., 2014b). On one hand, the humid–hot cities (i.e., the southern and eastern regions) normally had higher soil moisture content (increase heat storage) than arid–cold cities (i.e., the Northwest) (Chow and Roth, 2006). Consequently, the wet cities generally promote larger urban–rural gradient in soil moisture than dry cities, resulting in lower ΔT in urban zones compared to rural reference at night. The significant negative relationship between nighttime ΔT changing rates and climatic factors in spite of the season provides strong support for this argument (Table 1). Cities located in East China demonstrated the lowest rates, possibly because the "non-built-up" land for those cities are dominated by rice paddy fields or other wetlands with no water limitation that can largely increase rural heat storage (Hao et al., 2015). At the same time, the southeastern cities, mainly covered by evergreen forests and continuous cropland, had lower surface albedo and thus reduced heat loss through increasing heat storage in rural areas than northwestern neighbors (Jin et al., 2005; Zhou et al., 2014b).

Table 1
Pearson's correlation coefficients between the linear changing rates of urban heat island effect (ΔT) along the Urban Development Intensity (UDI) gradients and the climatic (precipitation and temperature) or background vegetation [as reflected by rural Enhanced Vegetation Index (EVI)] factors across cities.

		Temperature	Precipitation	Background EVI
Day	Annual	0.46[a]	0.57[a]	0.59[a]
	Summer	−0.17	−0.34	0.37[b]
	Winter	0.65[a]	0.57[a]	0.51[a]
Night	Annual	−0.60[a]	−0.70[a]	−0.43[b]
	Summer	−0.60[a]	−0.42[b]	−0.48[a]
	Winter	−0.61[a]	−0.71[a]	−0.50[a]

[a] Significant at 0.01 level.
[b] Significant at 0.05 level.

Large seasonal changes of the ΔT–UDI trends with evident spatial distributions were observed for the 32 cities. In the daytime, the ΔT increased more rapidly in summer than in winter for nearly all the cities (Figs. 3, 4B, and C), mainly because of the stronger evaporative cooling effects produced by vegetated surface in summer than in winter (Imhoff et al., 2010; Jin, 2012; Zhou et al., 2014b). The northern parts of China witnessed larger seasonal changes, which can be attributed to the greater seasonal change of the vegetation activity in the regions (caused by intensive agricultural practices in summer and defoliation in winter) (Piao et al., 2003). Conversely, the ΔT trend was much weaker in summer than in winter for the cities in North and Northeast China during the night (Figs. 4–6). Three factors might contribute to this phenomenon. First, the albedo differences between urban and rural areas were more pronounced during winter than summer because of defoliation and/or snow and ice coverage for most cities, particularly for the high-latitude cities (Zhou et al., 2014b), which in turn increased the ΔT in winter. Second, lower soil moisture in winter than in summer, influenced by the monsoon climate (Wu et al., 2005), could drive more rapid increase of ΔT with UDI in winter than in summer by reducing heat storage and subsequently releasing heat at night in the rural zones. Finally, the heating-created anthropogenic heat flux in urban areas during winter, especially for the high-latitude cities where central heating systems are used extensively, could indirectly strengthen the ΔT trends (Zhou et al., 2014b).

Exceptions to above-mentioned patterns were observed. For example, one arid land-locked city (i.e., Lanzhou) exhibited a clear temperature decline trend, the "cold island effect", along the UDI gradients in the daytime in the summer (Fig. 3). This is possibly due to the cooling

Table 2
Linear regression examining the temporal trends of rural land surface temperature (T_r) and the ΔT in urban zones (i.e., exurban, suburban, urban, and urban core) relative to the base rural condition for China's 32 major cities from 2003 to 2012.

City	Daytime					Nighttime				
	T_r	Exurban	Suburban	Urban	Urban core	T_r	Exurban	Suburban	Urban	Urban core
Beijing	−0.12[b]	0.06[a]	0.07[a]	0.07[b]	0.06	−0.09	0.02[a]	0.03[a]	0.04[a]	0.04[b]
Changchun	−0.23	−0.02[a]	−0.03	−0.02	−0.03	−0.19	0.00	0.02[b]	0.06[a]	0.10[a]
Changsha	−0.09	−0.01	0.03	0.03	0.06	−0.07	−0.01	−0.00	−0.02	0.03
Chengdu	−0.03	0.09[b]	0.10[b]	0.07	−0.03	0.11[b]	−0.06	−0.07	−0.06	−0.08
Chongqing	−0.11	0.05	0.09	0.03	−0.02	−0.02	0.07	0.07	0.02	−0.06
Fuzhou	−0.21[a]	−0.01	0.01	0.01	−0.07	−0.03	−0.01	−0.02	−0.04	0.04
Guangzhou	−0.12[b]	0.06[a]	0.07[b]	0.07	0.04	−0.04	0.01	0.02	0.04	0.04
Guiyang	−0.08	0.03	0.03	0.00	−0.00	−0.17[b]	0.03	0.12	0.10	0.06
Haikou	−0.20[a]	0.04	0.08[b]	0.08	0.08	0.14[b]	−0.03	−0.03	−0.08	−0.07
Hangzhou	−0.22[b]	0.05[b]	−0.00	−0.01	−0.07	−0.08	−0.02	−0.03	−0.02	−0.05
Harbin	−0.19	0.00	0.00	0.01	−0.00	−0.15	−0.02	0.01	0.03	0.06
Hefei	−0.05	0.02	0.06[b]	0.04	−0.07	−0.11[b]	−0.02	−0.03	0.06	0.07
Hohhot	0.15	−0.04	−0.09[b]	−0.13[b]	−0.21[a]	−0.04	0.02	0.06[a]	0.08[b]	0.07
Jinan	−0.02	0.00	0.01	0.02	−0.03	−0.11[b]	0.00	0.03[b]	0.06[a]	0.06[b]
Kunming	0.08	0.04	0.01	−0.02	−0.12	0.03	−0.01	0.01	−0.01	−0.01
Lanzhou	−0.04	−0.03	−0.03	−0.04	−0.04	−0.07[b]	0.01	0.01	0.00	0.01
Lhasa	0.27	−0.03	−0.08	−0.14[b]	−0.09	0.06	0.03[b]	0.13[a]	0.13[a]	0.22[a]
Nanchang	−0.10	0.00	−0.04	−0.06	−0.10	−0.08[b]	0.02	0.01	−0.02	−0.03
Nanjing	−0.07	0.03[a]	0.10[b]	0.04	−0.03	−0.09[a]	0.00	0.01	0.02	0.03
Nanning	−0.19[b]	0.05	0.11[a]	0.13[b]	0.08	−0.09[b]	0.02	0.05	0.13	0.11
Shanghai	−0.06	−0.02	−0.05	−0.09[a]	−0.10[b]	−0.11[b]	0.03[b]	0.05[b]	0.06[a]	0.05[b]
Shenyang	−0.30	0.04[a]	0.11[a]	0.14[a]	0.12[a]	−0.04	0.01	−0.00	0.01	0.00
Shenzhen	−0.12[b]	0.03	0.04	0.04	0.01	−0.05	0.00	−0.00	0.02	0.01
Shijiazhuang	−0.01	0.02	0.04[b]	0.03	−0.07	0.48[b]	0.01[a]	0.02[a]	0.05[a]	0.05[b]
Taiyuan	−0.23[b]	0.07[a]	0.10[a]	0.09[b]	0.09	−0.11[b]	0.01	0.03[b]	0.05[a]	0.07[b]
Tianjin	−0.10	0.01	0.06[a]	0.11[a]	0.08[a]	−0.08	0.00	0.00	0.01	0.02
Urumqi	−0.03	0.00	−0.05	−0.08	0.06	−0.08	0.04[b]	0.05[b]	0.05	0.05
Wuhan	−0.07	0.05	0.04	−0.03	−0.10	−0.07	0.00	−0.00	−0.05	−0.05
Xi'an	−0.06	0.01	0.04	0.04	−0.00	−0.09	0.00	0.03[b]	0.05	0.05
Xining	−0.06	−0.00	−0.03	−0.10	−0.13[b]	−0.12[b]	0.03[a]	0.05[a]	0.08[a]	0.08[b]
Yinchuan	−0.10	0.05[a]	0.03	−0.07	−0.07	−0.03	−0.01[b]	0.03[b]	0.06[b]	0.06
Zhengzhou	0.01	0.02	0.11[b]	0.11	0.06	−0.10	0.01	0.06	0.07	0.08

[a] Significant at 0.01 level.
[b] Significant at 0.05 level.

effects of plant evapotranspiration induced by the relatively higher vegetation activity and soil moisture (by irrigation) in urban zones compared to rural areas. In addition, two arid cities (Lanzhou and Urumqi) presented cold island effects during the day in winter. This might be related to the air pollution (Zhou et al., 2014b) and vegetation activity in this season. Heavy air pollution in winter for the northern cities resulted from large amount of coal burned for heating (He et al., 2002) can decrease incoming solar radiation in the urban area compared to the rural area (Sang et al., 2000), which in turn might artificially reduce urban temperature and even result in cold island effect. Low vegetation activity in winter exerted little cooling effects on rural surface, where usually there is more available energy than its urban counterpart during the day (Li and Bou-Zeid, 2013). This could result in urban cold island in those cities as well. Moreover, two humid–hot cities (Nanjing and Hefei) showed cold island effect in exurban and suburban areas compared to rural references, likely due to the abundance of surface water in the rice paddy fields or other wetlands in these rural areas (Hao et al., 2015).

We also found that the ΔT trends were not always in linear forms. Convex and concave patterns were formed under certain natural and anthropogenic influences. For example, some northern cities presented a concave trend in the daytime during summer mainly because of the higher evapotranspiration (cooling effects) per vegetated surface in exurban and/or suburban areas compared to rural counterparts induced by intensive land use activities (e.g., agricultural practices and urban green land management) (Piao et al., 2003; Zhou et al., 2014a). The concave trend was also found at night for some northern cities. The reason for this phenomenon was not clear. It might be related to the lower heat storage and releasing per impervious surface in exurban and/or suburban areas (mostly residential area) compared to urban core zones (mainly commercial area) (Oke, 1982). In contrast, two southern cities (Kunming and Shenzhen) showed a convex increase in the day primarily due to the higher evapotranspiration per vegetated pixels in urban and urban core areas caused by intensive urban greening practices (Zhou et al., 2014a). At the same time, two arid cities (Lanzhou and Lhasa) exhibited convex increase at night, possibly because the influence of water body in the cities. There were rivers cross exurban and suburban zones of the two cities. This could increase heat storage during the day and thus might promote the ΔT in the areas (i.e., exurban and suburban) close to the river (e.g., Oke, 1982).

4.2. Temporal trends of the UHI effects from 2003 to 2012 in China

We found that the background temperature (as reflected by rural land surface temperature) decreased from 2003 to 2012 for most cities (Table 2), closely related to the trends of air temperature (Table S2). The ΔT, however, increased significantly in about one-third of the cities, especially in the suburban areas during both the day and night times (Table 2). These can be attributed to a) more built-up land expansion occurred in the suburban area over time (Fig. 7), and b) more intensive management of urban green space in the urban and urban core areas (Zhou et al., 2014a). Conversely, few cities showed apparent decline trends of daytime ΔT in urban or urban core zones (Table 2) even though they experienced simultaneous urbanization intensification (Fig. 7). The improved management and maintenance of urban green spaces likely drove part of this relationship. Chinese municipal governments have created new green areas or preserved existing green spaces in conjunction with rapid urbanization in recent years (Yu and Padua, 2007; Zhao et al., 2013).

We found that the inter-annual variations of the ΔT were generally invariant with climate factors (Table S2). Nevertheless, few cities with significant correlations indicated that more intensive ΔT was likely to

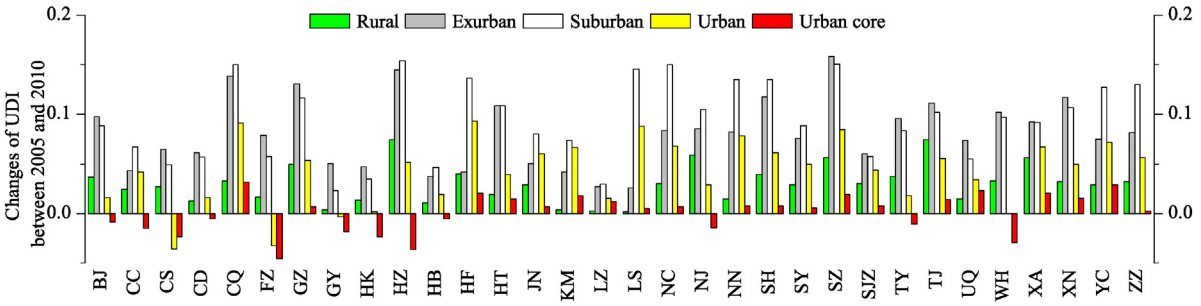

Fig. 7. Changes of the mean UDI in different UDI zones from 2005 to 2010.

happen in wet years during the day (i.e., positive relationship) and in dry years for the night (i.e., negative relationship) (Table S2). This phenomenon can be explained by the better vegetation condition and the higher soil moisture content during the wet years that can result in larger daytime ΔT and lower nighttime ΔT compared to the dry years. Surprisingly, weaker surface UHI effects were more likely to occur in hot years during both the day and night times (Table S2), contrary to the previous understanding that heat waves could accelerate UHI effects due to the associated decrease of surface moisture and wind speed in urban areas (Li and Bou-Zeid, 2013). The discrepancy might be attributed to 1) the satellite data available is not long enough to reflect the relationship between UHI and climate variability (Zhao et al., 2014), and 2) the collinearity problem of the climatic impacts with that induced by other factors (Zhou et al., 2014b). Long-term observations and physical-based models are urgently needed to investigate the responses of UHI effects to climate extremes in future.

4.3. Caution to the methods to quantify UHI intensity over large areas

The varying ΔT trends along UDI gradients across space and time suggests that caution should be paid to the methods to quantify UHI intensity over large areas. For example, the annual mean UHI intensity, if defined as temperature differences in urban and urban core (UDI > 0.5) relative to rural (UDI < 0.05) areas in current research, reached up to 2.20 °C in the day and 2.17 °C at night for those 32 major cities (Fig. 8). These two values are nearly two times as large as our previous estimates (1.11 and 1.13 °C for the day and night, respectively) that were loosely defined as the temperature differences between urban (UDI > 0.5) and nearby equal-area buffer zones (Zhou et al., 2014b). The direction of the UHI estimates might be reversed when using different methods. For example, two arid cities (Lanzhou and Urumqi) exhibited cold island effect in this analysis but had weak heat island effect if compared to suburban during the day on an annual mean scale. The relative magnitudes of the UHI effect across regions might also differ if the quantification method is used. For example, the greatest daytime and nighttime UHI intensity happened in East and Northwest China, respectively, yet both occurred in Northeast China if compared to suburban areas. It is therefore necessary to realize the empirical nature of the estimated UHI intensities because of their dependence on the definitions. However, UHI estimates under the two definitions were positively and significantly related, especially for the diurnal changes (Table 3). For example, the UHI intensity was higher in summer than winter for most cities during the day, with the opposite for the night (Fig. 8), which was highly consistent with our previous

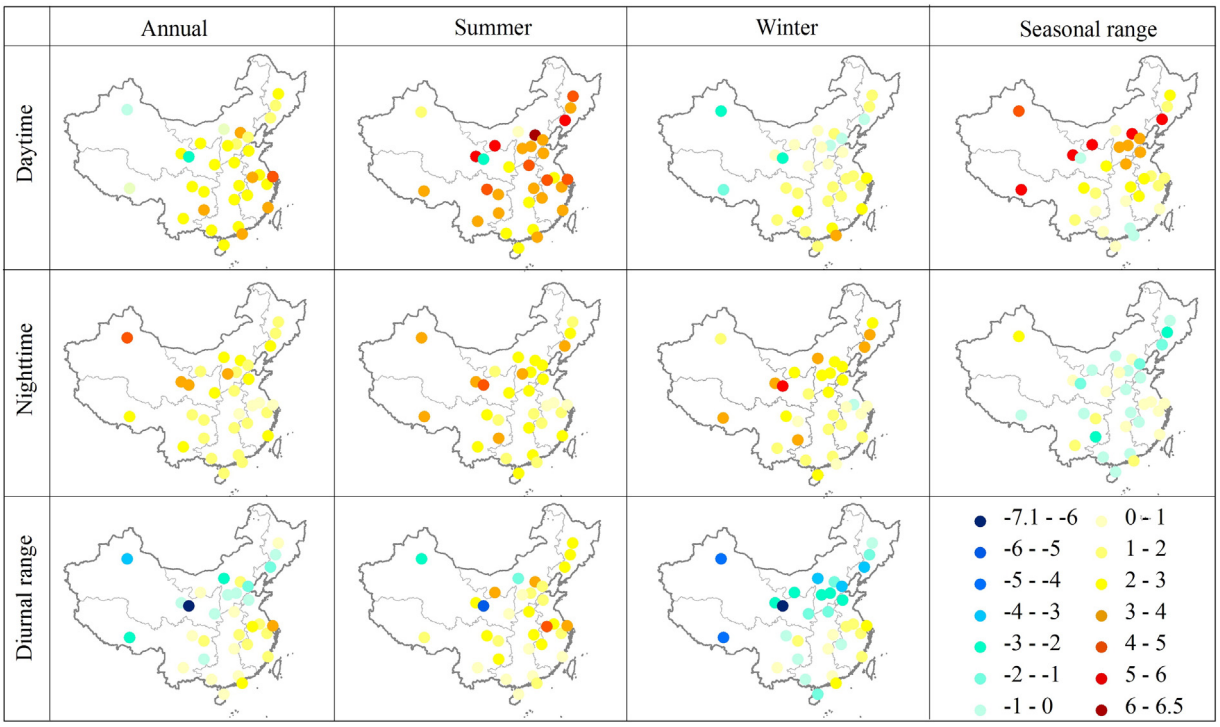

Fig. 8. Spatial distributions of surface urban heat island intensity (°C) in China's 32 major cities averaged over the period 2003–2012. The diurnal and seasonal ranges were defined as the intensity differences between daytime and nighttime and between summer and winter, respectively.

findings (Zhou et al., 2014b). This phenomenon can be attributed to the fact that the large-scale UHI distribution was largely controlled by the background climate (Imhoff et al., 2010; Zhou et al., 2014b, Zhao et al., 2014).

4.4. Uncertainties

Uncertainties remain in this analysis. First, large area differences existed among UDI zones for a particular city and across cities, which may affect the area-weighted mean LST. Second, we used the empirical value of the rural LST to represent city's climatic background, and assumed that there were no urbanization effects in rural areas. Our results did show that the UDI in the rural zone increased slightly over time for all the cities (Fig. 7), which suggest that the UHI effect (difference relative to rural areas) might be underestimated. Third, we did not conduct a detailed attribution analysis on the phenomenon that both the convex and concave ΔT–UDI trends have been observed in few cities. It might be related to the intensified vegetation management (e.g., irrigation, fertilization, choice of species) and the existence of water body. However, other factors such as landscape configuration (Arnfield, 2003; Li et al., 2011; Oke, 1982), atmospheric environment(Jauregui and Luyando, 1999), and land use (Jin et al., 2005; Oke, 1982) may play important roles in forming these trends. Fourth, cold island effect happened in a few cities, especially during the daytime in the winter. The actual reason for this phenomenon remains unclear. Fifth, although urbanization intensified through time, more than half of the cities demonstrated insignificant trends of the ΔT, likely because our research period was not long enough to adequately reflect the temporal trends. Moreover, we used the static land coverage maps in 2005 and 2010 (Zhao et al., 2015) to delineate the UDI maps for the periods of 2003–2007 and 2008–2012, respectively. This would introduce some biases on the UDI distribution, especially for cities that experienced rapid urbanization. In future projects, consecutive land-cover maps would likely result in a more effective evaluation of the ΔT trends over time.

5. Conclusions

This study examined the spatiotemporal trends of surface UHI effects (i.e., ΔT) along the UDI gradient in 32 major cities across different regions of China. Since China has complex zonal variations and experienced the world's most intensive urbanization in recent decades, this analysis provides valuable information on predicting the UHI effects and the associated consequences in the context of future urban development over large areas.

Our results indicated that both the daytime and nighttime ΔT increased dramatically with a rising UDI for majority of cities, with a great deal of spatial heterogeneities. Larger intensifying rates were observed in the southeastern and northwestern portion of China for the day and night, respectively. At the same time, the ΔT–UDI relationships were not always linear, convex and concave patterns can be formed under certain natural and anthropogenic influences. In addition, we indicated that the ΔT trends differed greatly by season, characterized by the higher increasing rates in summer during the day and in winter at night across most cities. The background climate-vegetation regimes were found mainly responsible for the ΔT–UDI trends across cities, while human activities and the agricultural practices in particular also matters. Inter-annually, we showed that the ΔT increased significantly in about one-third of the cities in the past decade (especially in suburban areas) and decreased in few cases. These patterns, however, were mainly controlled by human activities such as the urban development and urban green space management, and were overall invariant with local climate variability.

This research highlights the strong and highly diverse urbanization effects on local climate, stressing the necessity of the site-specific mitigation actions for sustainable urban development. Also, we emphasize that caution should be paid to the methods to quantify UHI effects over large areas, since the UHI estimate may vary substantially by the definitions and the direction can even be reversed. Nevertheless, the impacts of urbanization on climate are complex and uncertainties remained in this study. While remote sensing is helpful in quantifying the UHI effects over large areas, the combination use of direct observations and earth system models are needed for a better understanding of the physical characteristics, driving forces, and consequences of UHI, and therefore help formulating the climate mitigation strategies and plans.

Table 3
Pearson's correlation coefficients between the urban heat island intensities as estimated in this study and that in our previous research (Zhou et al., 2014b) for China's 32 major cities.

	Annual	Summer	Winter	Seasonal change
Daytime	0.58[a]	0.58[a]	0.41[b]	0.51[a]
Nighttime	0.42[b]	0.54[a]	0.55[a]	0.38[b]
Diurnal change	0.66[a]	0.70[a]	0.65[a]	–

[a] Significant at the 0.01 level (2-tailed).
[b] Significant at the 0.05 level (2-tailed).

Acknowledgements

This study was supported by the National Natural Science Foundation of China (#41501465), the Natural Science Foundation of the Jiangsu Higher Education Institutions of China (#15KJB170013), and the Startup Foundation for Introducing Talent of NUIST (2014r051). We thank Dr. Johnny Boggs (Eastern Forest Environmental Threat Assessment Center, USDA Forest Service Southern Research Station) and three anonymous reviewers for their valuable comments to improve this manuscript.

Appendix A. Supplementary data

Supplementary data to this article can be found online at http://dx.doi.org/10.1016/j.scitotenv.2015.11.168.

References

Angel, S., Parent, J., Civco, D.L., Blei, A., Potere, D., 2011. The dimensions of global urban expansion: estimates and projections for all countries, 2000–2050. Prog. Plan. 75, 53–107.
Arnfield, A.J., 2003. Two decades of urban climate research: a review of turbulence, exchanges of energy and water, and the urban heat island. Int. J. Climatol. 23, 1–26.
Chan, K.W., 2010. Fundamentals of China's urbanization and policy. China Rev. 10, 63–93.
Chen, J., Jönsson, P., Tamura, M., Gu, Z., Matsushita, B., Eklundh, L., 2004. A simple method for reconstructing a high-quality NDVI time-series data set based on the Savitzky–Golay filter. Remote Sens. Environ. 91, 332–344.
Chow, W.T.L., Roth, M., 2006. Temporal dynamics of the urban heat island of Singapore. Int. J. Climatol. 26, 2243–2260.
Clinton, N., Gong, P., 2013. MODIS detected surface urban heat islands and sinks: global locations and controls. Remote Sens. Environ. 134, 294–304.
Dixon, P.G., Mote, T.L., 2003. Patterns and causes of Atlanta's urban heat island-initiated precipitation. J. Appl. Meteorol. 42, 1273–1284.
Foody, G.M., 2002. Status of land cover classification accuracy assessment. Remote Sens. Environ. 80, 185–201.
Gong, P., Liang, S., Carlton, E.J., Jiang, Q., Wu, J., Wang, L., Remais, J.V., 2012. Urbanisation and health in China. Lancet 379, 843–852.
Gregg, J.W., Jones, C.G., Dawson, T.E., 2003. Urbanization effects on tree growth in the vicinity of New York City. Nature 424, 183–187.
Grimm, N.B., Faeth, S.H., Golubiewski, N.E., Redman, C.L., Wu, J., Bai, X., Briggs, J.M., 2008. Global change and the ecology of cities. Science 319, 756–760.
Hao, L., Sun, G., Liu, Y., 2015. Urbanization dramatically altered the water balances of a paddy field dominated basin in Southern China. Hydrol. Earth Syst. Sci. 12, 1941–1972.
He, K., Huo, H., Zhang, Q., 2002. Urban air pollution in China: current status, characteristics, and progress. Annu. Rev. Energy Environ. 27, 397–431.
Imhoff, M.L., Bounoua, L., DeFries, R., Lawrence, W.T., Stutzer, D., Tucker, C.J., Ricketts, T., 2004. The consequences of urban land transformation on net primary productivity in the United States. Remote Sens. Environ. 89, 434–443.
Imhoff, M.L., Zhang, P., Wolfe, R.E., Bounoua, L., 2010. Remote sensing of the urban heat island effect across biomes in the continental USA. Remote Sens. Environ. 114, 504–513.

IPCC, 2014. Climate Change: Impacts, Adaptation, and Vulnerability. Cambridge University Press, Cambridge, United Kingdom and New York, USA.
Jauregui, E., Luyando, E., 1999. Global radiation attenuation by air pollution and its effects on the thermal climate in Mexico City. Int. J. Climatol. 19, 683–694.
Jin, M., Shepherd, J.M., King, M.D., 2005. Urban aerosols and their variations with clouds and rainfall: A case study for New York and Houston. J. Geophys. Res. 110, D10S20.
Jin, M.S., 2012. Developing an index to measure urban heat island effect using satellite land skin temperature and land cover observations. J. Clim. 25, 6193–6201.
Jönsson, P., Eklundh, L., 2004. TIMESAT—a program for analyzing time-series of satellite sensor data. Comput. Geosci. 30, 833–845.
Li, D., Bou-Zeid, E., 2013. Synergistic interactions between urban heat islands and heat waves: the impact in cities is larger than the sum of its parts. J. Appl. Meteorol. Climatol. 52, 2051–2064.
Li, J., Song, C., Cao, L., Zhu, F., Meng, X., Wu, J., 2011. Impacts of landscape structure on surface urban heat islands: a case study of Shanghai, China. Remote Sens. Environ. 115, 3249–3263.
Oke, T.R., 1973. City size and the urban heat island (1967). Atmos. Environ. 7, 769–779.
Oke, T.R., 1982. The energetic basis of the urban heat island. Q. J. R. Meteorol. Soc. 108, 1–24.
Patz, J.A., Campbell-Lendrum, D., Holloway, T., Foley, J.A., 2005. Impact of regional climate change on human health. Nature 438, 310–317.
Peng, S., Piao, S., Ciais, P., Friedlingstein, P., Ottle, C., Bréon, F.M., Nan, H., Zhou, L., Myneni, R.B., 2012. Surface urban heat island across 419 global big cities. Environ. Sci. Technol. 46, 696–703.
Piao, S., Fang, J., Zhou, L., Guo, Q., Henderson, M., Ji, W., Li, Y., Tao, S., 2003. Interannual variations of monthly and seasonal normalized difference vegetation index (NDVI) in China from 1982 to 1999. J. Geophys. Res. 108, 4401.
Reid, W.V., 1998. Biodiversity hotspots. Trends Ecol. Evol. 13, 275–280.
Sang, J., Liu, H., Liu, H., Zhang, Z., 2000. Observational and numerical studies of wintertime urban boundary layer. J. Wind Eng. Ind. Aerodyn. 87, 243–258.
Searle, S.Y., Turnbull, M.H., Boelman, N.T., Schuster, W.S., Yakir, D., Griffin, K.L., 2012. Urban environment of New York City promotes growth in northern red oak seedlings. Tree Physiol. 32, 389–400.
Seto, K.C., Güneralp, B., Hutyra, L.R., 2012. Global forecasts of urban expansion to 2030 and direct impacts on biodiversity and carbon pools. Proc. Natl. Acad. Sci. 109, 16083–16088.
Shepherd, J.M., 2005. A review of current investigations of urban-induced rainfall and recommendations for the future. Earth Interact. 9, 1–27.
Storey, J., Scaramuzza, P., Schmidt, G., Barsi, J., 2005. Landsat 7 scan line corrector-off gap filled product development. Proceedings of Pecora, pp. 23–27.
Strahler, A.H., 1980. The use of prior probabilities in maximum likelihood classification of remotely sensed data. Remote Sens. Environ. 10, 135–163.
United Nations, 2014. Department of Economic and Social Affairs, Population Division. World urbanization prospects: The 2014 revision, New York: NY, United Nations 2014.
Wan, Z., 2008. New refinements and validation of the MODIS land-surface temperature/emissivity products. Remote Sens. Environ. 112, 59–74.
Wan, Z., Dozier, J., 1996. A generalized split-window algorithm for retrieving land-surface temperature from space. IEEE Trans. Geosci. Remote Sens. 34, 892–905.
Wu, S., Yin, Y., Zheng, D., Yang, Q., 2005. Aridity/humidity status of land surface in China during the last three decades. Sci. China Ser. D Earth Sci. 48, 1510–1518.
Yu, K., Padua, M.G., 2007. China's cosmetic cities: urban fever and superficiality. Landsc. Res. 32, 255–272.
Yuan, F., Bauer, M.E., 2007. Comparison of impervious surface area and normalized difference vegetation index as indicators of surface urban heat island effects in Landsat imagery. Remote Sens. Environ. 106, 375–386.
Zhao, J., Chen, S., Jiang, B., Ren, Y., Wang, H., Vause, J., Yu, H., 2013. Temporal trend of green space coverage in China and its relationship with urbanization over the last two decades. Sci. Total Environ. 442, 455–465.
Zhao, L., Lee, X., Smith, R.B., Oleson, K., 2014. Strong contributions of local background climate to urban heat islands. Nature 511, 216–219.
Zhou, D., Zhao, S., Liu, S., Zhang, L., 2014a. Spatiotemporal trends of terrestrial vegetation activity along the urban development intensity gradient in China's 32 major cities. Sci. Total Environ. 488, 136–145.
Zhou, D., Zhao, S., Liu, S., Zhang, L., Zhu, C., 2014b. Surface urban heat island in China's 32 major cities: spatial patterns and drivers. Remote Sens. Environ. 152, 51–61.
Zhou, D., Zhao, S., Zhang, L., Sun, G., Liu, Y., 2015. The footprint of urban heat island effect in China. Sci. Report. 5, 11160.
Zhao, S., Zhou, D., Zhu, C., Qu, W., Zhao, J., Sun, Y., Huang, D., Wu, W., Liu, S., 2015. Rates and patterns of urban expansion in China's 32 major cities over the past three decades. Landsc. Ecol. http://dx.doi.org/10.1007/s10980-015-0211-7.